Dielectric relaxation and the molecular motion of poly(vinylidene fluoride) crystal form II under high pressure

Yoshihisa Miyamoto
Department of Physics, Faculty of Science, Kyoto University, Kyoto, 606 *Japan*
(*Received* 2 *November* 1982; *revised* 1 *April* 1983)

The α dielectric relaxation of poly(vinylidene fluoride) crystal form II is studied under pressures up to 7 kbar at temperatures from 100° to 200°C. The isotherm for variation of the dielectric increment with pressure shows a maximum. This behaviour is examined on the basis of models of molecular motion for the α relaxation previously proposed; longitudinal disorder exists in the crystalline chains. The calculations reproduce the experimental results except for the pressure coefficient of the dielectric increment. The metastable conformation exists together with the most stable conformation in one chain, and dipole reversal parallel to the molecular axis occurs throughout the whole chain.

Keywords Poly(vinylidene fluoride); dielectric relaxation; pressure; molecular motion; dipole; defect

INTRODUCTION

Dielectric relaxation due to molecular motion of polymer chains constrained in crystalline fields has been analysed mainly by the site model[1], which was originally proposed by Hoffman and Pfeiffer for long-chain compounds[2]. The limitation of the application of the site model to polymeric substances is not still clear. Recently, Boyd *et al.*[3,4] showed that neither the Onsager–Kirkwood equation nor the simple site model could explain the temperature dependence of the dielectric increment in polyethylene; the dielectric increment decreases with temperature faster than as the reciprocal of the absolute temperature. They argued that this temperature dependence should be due to the defects in the crystalline chains participating in the relaxation process.

In a previous paper[5], we ascertained that the α dielectric relaxation of poly(vinylidene fluoride) (PVDF) involves only the component of the dipole moment parallel to the molecular axis and that the defects in the crystalline region play an important role in the relaxation. We proposed two possible models for the dipolar orientation. However, the size of the motional unit and the role of defects are not still clarified.

In the present paper, the ionic contributions in the low-frequency region were reasonably subtracted by the method developed recently. Then α relaxation was studied over a wider temperature range under pressures higher than atmospheric pressure; the melting point increases with pressure. The dielectric increment–pressure curve showed a maximum at constant temperature, which is not expected from the simple site model. The molecular motion associated with α relaxation is clarified by taking account of the pressure and temperature dependence of the dielectric increment based on the models previously proposed.

EXPERIMENTAL

The material used was KF-polymer no. 1000 supplied by Kureha Chemical Ind. Ltd. The material was melted in vacuum at 220°C and slowly cooled to room temperature. Then the sample was annealed at 160°C for two days in order to avoid annealing effects during the dielectric measurements.

The crystal form of the sample was determined by wide-angle X-ray diffraction to be form II and no orientation was observed. The long period was 150 Å determined by small-angle X-ray scattering. The density was 1.797 g cm^{-3} at 20°C and the degree of crystallinity χ is estimated at about 0.6 after the data of Nakagawa and Ishida[6].

The dielectric measurements were carried out with a transformer bridge (Fujisoku DLB1102A) over the frequency range from 10^2 to 3×10^5 Hz at temperatures from 100° to 200°C and under pressures up to 7 kbar. The changes in the long period and the density before and after the dielectric measurements were not detected within the experimental error.

The high-pressure cell (Hikari Kikai Ltd) used for the dielectric measurements is shown in *Figure 1*. The pressure-transmitting fluid was a silicone oil (Toshiba TSF451) and pressure was measured by a calibrated manganin gauge.

Silver was evaporated onto both surfaces of the sample to form electrodes of area 79.8 mm^2. The electrodes of evaporated films were so thin (1000 Å) that the size of the electrodes changes with temperature and pressure in the same way as the sample. Therefore, the number of dipoles to be considered in the present measurements remains constant: the constant number of dipoles contributes to the dielectric constant in the present case. Corrections for the cell constant were made as follows. The specific

0032-3861/84/010063-08$03.00
© 1984 Butterworth & Co. (Publishers) Ltd.

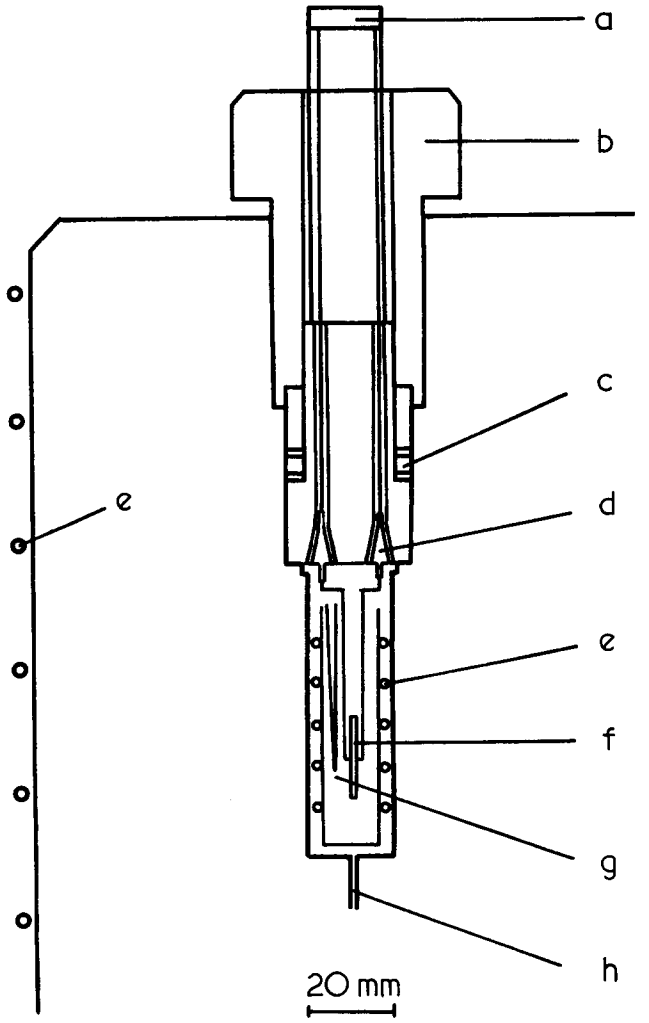

Figure 1 The high-pressure cell for dielectric measurements: (a) connector; (b) upper end plug; (c) packings; (d) terminals; (e) heater; (f) sample; (g) thermocouple; (h) inlet for oil

volume of the amorphous parts of PVDF in the present temperature and pressure region has not been reported so far. For the temperature dependence of the specific volume of the crystalline parts V_c and the amorphous parts V_a, the data of Nakagawa and Ishida[6] are used. The pressure coefficients of V_c and V_a are assumed to be independent of temperature and their pressure coefficients are adopted from the data of Tanaka *et al.*[7] at 150°C. The specific volume of the sample $V_s(t,P)$ at temperature t and pressure P is related to V_c and V_a by

$$V_s = \chi V_c + (1-\chi)V_a$$

and then given by:

$$V_s(t,0) = 0.555 + 1.86\times10^{-4}t + 4\times10^{-7}t^2 \quad (1a)$$

$$V_s(t,P) = V_s(t,0)(1 - 4.00\times10^{-2}P + 7.03\times10^{-3}P^2 - 5.47\times10^{-4}P^3) \quad (1b)$$

where t is temperature in degrees Celsius and P is pressure in kilobars. Then the cell constant $C(t,P)$ is expressed by:

$$\frac{C(t,P)}{C_0} = 1 + \frac{1}{3}\frac{V_s(t,P) - V_0}{V_0} \quad (2)$$

where C_0 and V_0 are the cell constant and the specific volume of the sample at room temperature and under atmospheric pressure, respectively. The maximum contribution from the second term in equation (2) is 0.019.

RESULTS

The frequency dependence of the dielectric constant ε' and dielectric loss ε'' at 180°C at various pressures is shown in *Figure 2*. The frequency at the loss maximum continuously decreases with increasing pressure up to 7 kbar; no sudden change in the relaxation mechanism occurs in this pressure range. The increase in ε' and ε'' in the low-frequency region is attributed to interfacial polarization and its frequency dependence is given by[8]:

$$\varepsilon_i'(\omega) = A\omega^{-m}\cos(\pi m/2)$$
$$\varepsilon_i''(\omega) = A\omega^{-m}\sin(\pi m/2) \quad (3)$$

where ω is angular frequency and A and m depend only on temperature and pressure ($0 \leqslant m \leqslant 1$). When, taking the data at 180°C as examples, we put $m = 0.6$ and the values of A are determined by a trial-and-error method, the contribution from interfacial polarization can be subtracted from the observed results. The resulting values of ε' and ε'', which can be regarded as the values of the α relaxation, are shown in *Figure 3*. In this figure, the dielectric constant is nearly constant at low frequency and the dielectric loss curves represent broad peaks typical of polymeric substances. The dielectric constant ε' and dielectric loss ε'' nearly obey the Cole–Cole circular law.

When it is assumed that the increase in ε' and ε'' at low frequency is expressed by equation (3) and that the resulting ε' and ε'' obey the Cole–Cole law, the observed values of ε' adn ε'' are expressed by:

$$\varepsilon'(\omega) = \varepsilon_\infty + \frac{\Delta\varepsilon\cos\phi}{\left[1 + e^{2\beta x} + 2e^{\beta x}\cos\frac{\pi\beta}{2}\right]^{1/2}} + A\omega^{-m}\cos\left(\frac{\pi m}{2}\right) \quad (4)$$

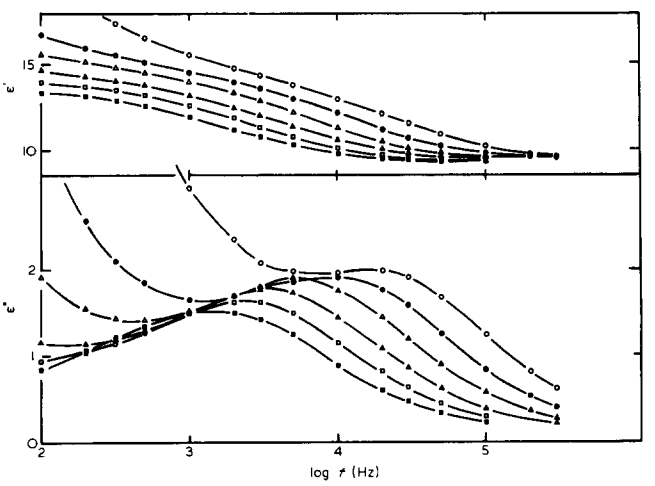

Figure 2 The frequency dependence of dielectric constant ε' and loss ε'' at 180°C under various pressures: ○, 2.0 kbar; ●, 3.0 kbar; △, 4.0 kbar; ▲, 5.0 kbar; □, 6.0 kbar; ■, 7.0 kbar. No correction is made for the cell constant in *Figures 2* and *3*

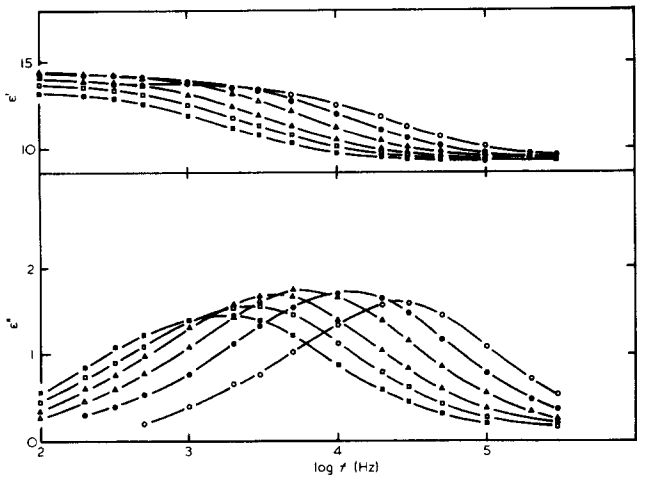

Figure 3 The contribution from the low-frequency process (interfacial polarization) is subtracted from the values in *Figure 2*. The symbols are the same as in *Figure 2*

$$\varepsilon''(\omega)=\frac{\Delta\varepsilon\sin\phi}{\left[1+e^{2\beta x}+2e^{\beta x}\cos\frac{\pi\beta}{2}\right]^{1/2}}+A\omega^{-m}\sin\left(\frac{\pi m}{2}\right)$$

where ε_∞ is the limiting value of the dielectric constant at high frequency, $\Delta\varepsilon$ is the dielectric increment, β is the Cole–Cole parameter representing the distribution of relaxation times, $x=\ln\omega\tau$ where τ is the principal relaxation time, and

$$\phi=\arctan\left(\frac{e^{\beta x}\sin(\pi\beta/2)}{1+e^{\beta x}\cos(\pi\beta/2)}\right)$$

By the least-squares method, the values of these parameters are determined at each temperature and pressure. The dielectric increment and the relaxation time thus obtained are shown in *Figures 4* and *5*. In the present ranges of temperature and pressure, the values of β are 0.70–0.78 and those of m are 0.58–0.62, and they do not depend significantly on temperature and pressure.

It is seen from *Figure 4* that, firstly, the dielectric increment–pressure curve shows a clear maximum above 120°C. Secondly, the pressure at which $\Delta\varepsilon$ reaches a maximum increases with increasing temperature. Thirdly, the peak value of $\Delta\varepsilon$ decreases with temperature. The activation volume can be obtained from *Figure 5*; it decreases from 30 to 20 $cm^3\ mol^{-1}$ with increasing temperature and also shows a slight pressure dependence. The activation enthalpy is obtained from a plot of $\log\tau$ vs $1/T$ and the activation internal energy is about 23 kcal mol^{-1}. These values roughly agree with the results of Sasabe[9] and Yano[10].

DISCUSSION

As in the previous paper[5], the temperature and pressure dependence of $\Delta\varepsilon$ is examined on the basis of the two-site model. The dielectric increment $\Delta\varepsilon$ is expressed by:

$$\Delta\varepsilon/x=\frac{4\pi}{3kT}KN\mu^2\,\mathrm{sech}^2\left(\frac{\Delta G}{2kT}\right) \qquad (5)$$

where k is the Boltzmann constant, T is the absolute temperature, N is the number of dipoles per cubic centimetre, μ is the component of the dipole moment parallel to the molecular axis, ΔG is the difference in the Gibbs free energy between the two sites and K is a correction factor including two factors, i.e. the ratio of the internal field to the applied field and the correction factor for taking the value of dipole moment in vacuum. When ΔU, ΔS and ΔV are the differences in the internal energy, the entropy and the volume between the two sites, respectively, ΔG is given by:

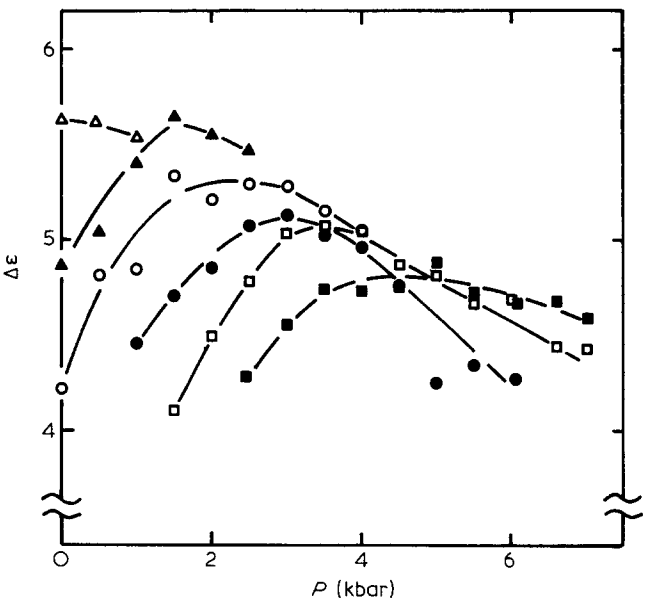

Figure 4 The pressure dependence of the dielectric increment at various temperatures: △, 100°C; ▲, 120°C; ○, 140°C; ●, 160°C; □, 180°C; ■, 200°C

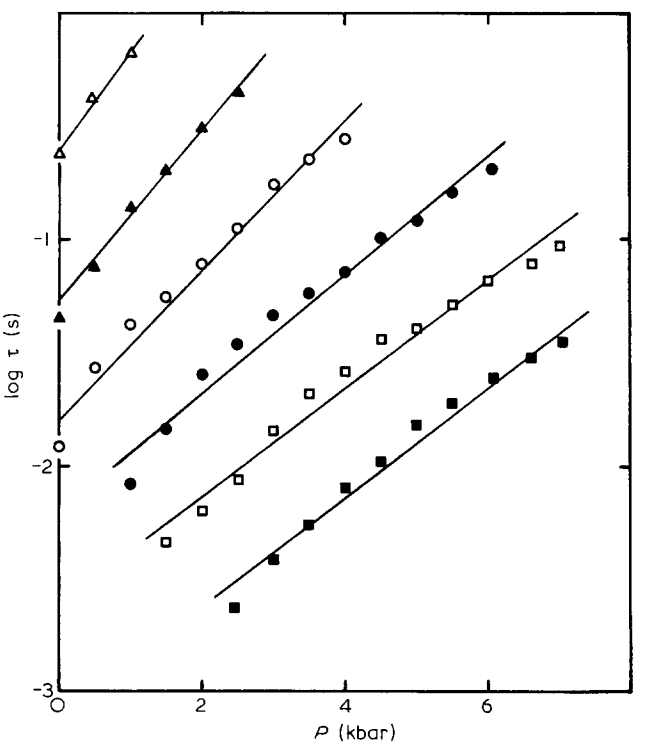

Figure 5 The pressure dependence of relaxation time. The symbols are the same as in *Figure 4*

$$\Delta G = \Delta U - T\Delta S + P\Delta V \quad (6)$$

As shown in the previous paper, the α relaxation involves only the polarization parallel to the molecular axis: dipole reversal due to conformation change from $TGT\bar{G}$ to $\bar{G}TGT$. As there is no entropy difference between the two sites due to the conformation, ΔS is assumed to be zero by neglecting the difference in the volume and the vibration in each site. Moreover, ΔU and ΔV are assumed to be positive and constant in the measured temperature and pressure range. Then, from equations (5) and (6) $\Delta\varepsilon$ will decrease with pressure for an isothermal process, though it may have a maximum with respect to temperature for an isobaric process.

For the Onsager internal field which is applicable to a spherical molecule, the term K is given by:

$$K = [(\varepsilon_\infty + 2)/3]^2 \, 3\varepsilon_0/(2\varepsilon_0 + \varepsilon_\infty)$$

where ε_0 is the limiting value of the dielectric constant at low frequency. It must be examined, however, whether a molecule can be approximated by a sphere or by an ellipsoid in accordance with the model of the molecular motion. In the following discussion, the temperature and pressure dependence of K is neglected.

Thermodynamics of dielectrics

In a dielectrically isotropic system, the Gibbs free energy G of the system is considered to be a function of temperature T, pressure P and electric field E. Its total differential can be expressed by the well known relation:

$$dG = -SdT + VdP - \frac{M}{4\pi}dE \quad (7)$$

where S is the entropy, V the volume and M the polarization of the system. For a system in which M is proportional to E, the dielectric increment $\Delta\varepsilon$ is given by M/E. From equation (7), we find for an isobaric and for an isothermal process, respectively, that:

$$\left(\frac{\partial S}{\partial(E^2)}\right)_{P,T} = \frac{1}{8\pi}\left(\frac{\partial(\Delta\varepsilon)}{\partial T}\right)_{P,E^2} \quad (8a)$$

and

$$\left(\frac{\partial V}{\partial(E^2)}\right)_{T,P} = -\frac{1}{8\pi}\left(\frac{\partial(\Delta\varepsilon)}{\partial P}\right)_{T,E^2} \quad (8b)$$

From the contour map of $\Delta\varepsilon$ shown in *Figure 6*, it is seen that, in region A, $\Delta\varepsilon$ increases with increasing temperature and decreasing pressure, while in region B, on the contrary, $\Delta\varepsilon$ decreases with increasing temperature and decreasing pressure. According to equations (8a) and (8b), both the entropy and the volume of the system increase by applying an electric field in region A. Therefore, in region A the system is in an ordered state for the orientation and the packing of dipoles, but in region B the system becomes a disordered state. However, the broken line in *Figure 6* separating the regions A and B does not necessarily imply a phase change from 'phase A' to 'phase B'; as mentioned above, even in the two-site model, which does not have a phase change at all, the sign of $\partial(\Delta\varepsilon)/\partial T$ changes with temperature.

Dielectric increment

For simplicity, let us consider the quantity $T\Delta\varepsilon/\chi$ instead of $\Delta\varepsilon/\chi$. According to the simple two-site model with definite potential wells, where N and μ are independent of temperature and pressure, $T\Delta\varepsilon/\chi$ is a measure of $\mathrm{sech}^2(\Delta G/2kT)$ and will increase with temperature and decrease with pressure.

From the experimental results shown in *Figure 4*, $T\Delta\varepsilon/\chi$ for the six isotherms versus pressure are plotted in *Figure 7* ($\chi = 0.6$). Above 120°C, $T\Delta\varepsilon/\chi$ reaches a maximum at pressure $P_{max}(T)$. The pressure $P_{max}(T)$ increases with increasing temperature. The peak value of $T\Delta\varepsilon/\chi$ increases slightly with temperature. In isobars at pressure between 1 and 4 kbar, $T\Delta\varepsilon/\chi$ also has a maximum at temperature $T_{max}(P)$, but the accuracy of $T_{max}(P)$ is not good because an isobar includes only five pressure points at most. The temperature dependence of $P_{max}(T)$ and the pressure dependence at $T_{max}(P)$ are shown in *Figure 8*. The relations $P_{max}(T)$ and $T_{max}(P)$ can be regarded as shown by the same straight line whose slope θ is 0.0378 kbar K^{-1} and which crosses the abscissa for $P = 0$ kbar at $T = 357$ K.

The experimental results obtained are not consistent with the behaviour predicted by the simple two-site model. We will thus analyse these data on the basis of the two models of molecular motion previously proposed[5], where N and/or μ depend(s) on temperature and pressure.

Here, brief explanations of the two models are given. $TGT\bar{G}$ conformation (hereafter referred to as up state or up segment) and $\bar{G}TGT$ conformation (down state) are considered to coexist in one chain in a lamella. In model 1, a conformational defect located at the boundary between up segment sequence and down one is activated thermally and moves along the molecular axis. This defect motion causes the reversal of dipole moments along the molecular axis. In this model the number of dipoles corresponds to that of the defects and the magnitude of the dipole moment is determined by the range in which the defects can move. In model 2, the location of the defects in a chain is fixed during the dipole reversal. Though the reversal of the dipole moment occurs throughout one chain, the total moment of a chain is the vector sum of the moments of all

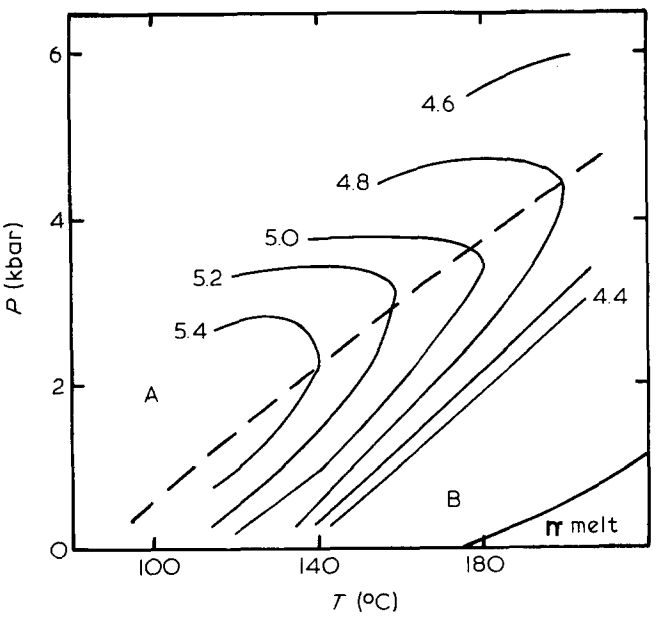

Figure 6 Contour map of the dielectric increment

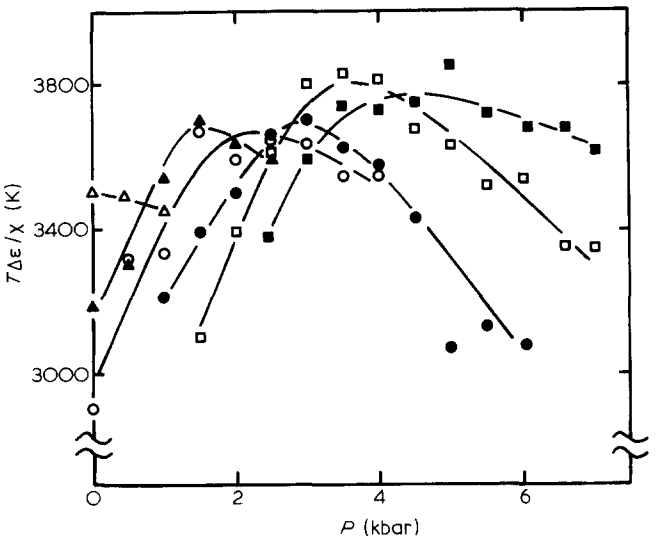

Figure 7 The pressure dependence of $T\Delta\varepsilon/\chi$. The symbols are the same as in *Figure 4*

the segments in a chain because up and down segments are mixed in a chain. Here, one segment corresponds to two monomers whose conformation is $TGT\bar{G}$ or $\bar{G}TGT$.

The defects under consideration are thermally created in a chain and the defect density should increase with increasing temperature and decreasing pressure. Though the molecular motion causing the α relaxation is also activated thermally, the lifetime of the defects is considered to be much longer than the relaxation times of the α relaxation. In the following discussion the density of defects is assumed to be an equilibrium value at a given temperature and pressure.

In model 1, the dipole moment can be assumed constant, i.e. the range of the defect movement is unaltered with temperature and pressure, but the number of dipoles (which is equal to the number of defects) increases with increasing temperature and decreasing pressure. Accordingly, the temperature and pressure dependence of $T\Delta\varepsilon/\chi$ cannot be explained by model 1.

In model 2, the number of dipoles, i.e. that of chains in crystalline lamellae, is constant, while the dipole moment (which is proportional to the difference in the number between up segments and down ones per chain) depends on the arrangements of up and down segments in a chain. The arrangements will depend on the energy difference

$$\Delta g = \Delta u - T\Delta s + P\Delta v$$

between up state (assumed the most stable conformation) and down state (thus, metastable one), and on the defect formation energy

$$W = U_1 - TS_1 + PV_1$$

Here, Δg, Δu, Δs and Δv are the differences in the Gibbs free energy, the internal energy, the entropy and the volume between up and down states and W, U_1, S_1 and V_1 are the Gibbs free energy, the internal energy, the entropy and the volume for defect formation, respectively. The difference in the entropy Δs between up ($TGT\bar{G}$) and down ($\bar{G}TGT$) states is assumed to be zero as in the case of ΔS. Moreover, the defects are assumed to be of TT conformation; we can put $S_1 = 0$.

As the defects exist at the boundaries between up segments sequences and down segments sequences, the difference in the number of up and down segments per chain becomes smaller as the number of defects increases. Then, the dipole moment μ decreases with increasing temperature and decreasing pressure. In the case in which the energy difference Δg between the two states is dominant in determining the arrangements, the ratio of the number of down segments to the number of up segments is expressed by $\exp(-\Delta g/kT)$; the dipole moment decreases with increasing temperature and decreasing pressure in this case, too. Both these effects bring about the reduction of the dipole moment with increasing temperature and decreasing pressure. Therefore, together with the term $\mathrm{sech}^2(\Delta G/2kT)$ in equation (5), $T\Delta\varepsilon/\chi$ will have a maximum with respect to both temperature and pressure in the case of model 2.

Since, in this way the observed maximum in $T\Delta\varepsilon/\chi$ with respect to temperature and pressure is qualitatively explained by model 2, we try to estimate those values of the parameters which give the observed $P_{max}(T)$ and $T_{max}(P)$.

Neglecting the size of the defects, we regard the arrangements of the segments in a chain to be described by the simple Markov process with two states, that is, up and down states. When the transition probability matrix is written as:

$$\mathbf{P} = \begin{pmatrix} 1-p & p \\ q & 1-q \end{pmatrix} \tag{9}$$

$T\Delta\varepsilon/\chi$ is given from equations (5) and (A.9):

$$\frac{T\Delta\varepsilon}{\chi} = \frac{4\pi}{3k} K N_0 \mu_0^2 \,\mathrm{sech}^2\left(\frac{\Delta G}{2kT}\right)\left[N_s\left(\frac{p-q}{p+q}\right)^2 + \frac{4pq(2-p-q)}{(p+q)^3} - \frac{1}{N_s}\frac{8pq(1-p-q)}{(p+q)^4}\left[1-(1-p-q)^{N_s}\right]\right] \tag{10}$$

where the dependence of ΔG on the arrangements is neglected. In these equations, $1-p$, p, q and $1-q$ are the transition probabilities for up–up, up–down, down–up and down–down successions, respectively, N_0 is the

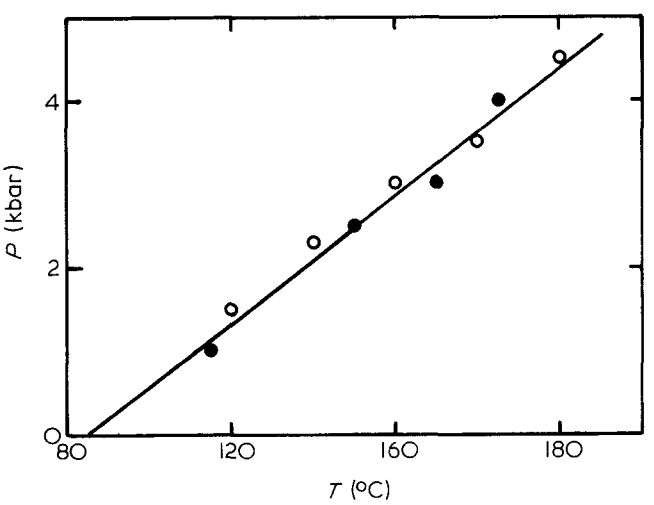

Figure 8 Relations of $P_{max}(T)$ and $T_{max}(P)$. Open circles indicate $P_{max}(T)$ obtained from *Figure 7* and full circles indicate $T_{max}(P)$

number of segments per unit volume (9.1×10^{21} cm^{-3}), μ_0 is the component of dipole moment of one segment parallel to the molecular axis (1.85 D) and N_s is the number of segments per chain. From the long period of 150 Å, the degree of crystallinity of 0.6 and the c-axis dimension of the unit cell of 4.92 Å,[11] N_s is estimated as about 20. The distribution of the lamellar thickness is neglected in deriving equation (10). In the square brackets in equation (10), the first term multiplied by N_s is the square of the average of the difference between the number of up segments and that of the down segments per chain and the second term represents the distribution around the average value.

When the defect density is given by the thermal equilibrium value, p and q are expressed in terms of Δg and W, but as there are six parameters to be determined, the following two extreme cases are examined.

Case (i): the energy difference Δg between up and down states is small enough to neglect the first term in the square brackets in equation (10). In this case, from equation (A.3), p and q are given by:

$$p=q=\frac{1}{1+\exp(W/kT)} \tag{11}$$

Case (ii): Δg is finite and the main contribution in the square brackets in equation (10) is $N_s[(p-q)/(p+q)]^2$. From equation (A.3), p and q are given by:

$$p=\frac{1}{1+\exp(\Delta g/kT)}$$
$$q=\frac{1}{1+\exp(-\Delta g/kT)} \tag{12}$$

In case (i), from equations (10) and (11), $T\Delta\varepsilon/\chi$ is given by:

$$T\Delta\varepsilon\chi=\frac{4\pi}{3k}KN_0\mu_0^2F(T,P) \tag{13}$$

where

$$F(T,P)\simeq\operatorname{sech}^2\left(\frac{\Delta G}{2kT}\right)\left(e^{W/kT}-\frac{e^{2W/kT}-1}{2N_s}\right) \tag{14}$$

The relations of $P_{max}(T)$ and $T_{max}(P)$ are obtained by differentiating $F(T,P)$ with respect to P and T, respectively:

$$P_{max(T)}:\ \left.\frac{\partial F(T,P)}{\partial P}\right|_{P=P_{max}}=0$$

and

$$T_{max}(P):\ \left.\frac{\partial F(T,P)}{\partial T}\right|_{T=T_{max}}=0$$

As both the relations $P_{max}(T)$ and $T_{max}(P)$ give the same linear function in the observed temperature and pressure range, i.e. around $P=0$ kbar and $T=T_0=357$K, the relations between parameters are obtained as follows:

$$V_1/\Delta V=U_1/\Delta U \tag{15}$$

$$\frac{\Delta U}{2kT_0}\tanh\left(\frac{\Delta U}{2kT_0}\right)=\frac{U_1}{2kT_0}\frac{e^{U_1/kT_0}-e^{2U_1/kT_0}/N_s}{e^{U_1/kT_0}-(e^{2U_1/kT_0}-1)/N_s} \tag{16}$$

$$\theta=U_1/T_0V_1 \tag{17}$$

where θ is the slope of the straight line in *Figure 8*. From equations (15), (16) and (17), when one of the parameters, for example U_1, is given, the other parameters, i.e. V_1, ΔU and ΔV, can be determined.

In model 2, one dipole corresponds to one chain. Then the value of K should be calculated for an ellipsoidal molecule with a distribution of dipole moments. If the dipole distribution is replaced by a mathematical dipole at the centre, K can be calculated from the formulae for the internal field and the reaction field of an ellipsoid[12,13] to be:

$$K=[1+(\varepsilon_\infty-1)A_1]^2\varepsilon_0/[\varepsilon_0+(\varepsilon_\infty-\varepsilon_0)A_1] \tag{18}$$

where

$$A_1=\frac{abc}{2}\int_0^\infty ds/(s+a^2)^{3/2}(s+b^2)^{1/2}(s+c^2)^{1/2} \tag{19}$$

and a, b and c are the semi-major axes of an ellipsoid ($a>b>c$). When an ellipsoid is approximated by a spheroid with the longest major axis given by the lamellar thickness (90 Å) and the other two major axes by the unit cell dimensions (4.9 Å for each), the value of K ranges from 1.14 to 1.15 for the α relaxation. The value of K is taken to be 1.14 in the numerical calculations of $T\Delta\varepsilon/\chi$.

By fitting the calculated values of $T\Delta\varepsilon/\chi$ to the experimental ones at P_{max}, we obtain the values of the parameters as $\Delta U=1.5$ kcal mol^{-1}, $\Delta V=4.4$ cm^3 mol^{-1}, $U_1=1.8$ kcal mol^{-1} and $V_1=5.4$ cm^3 mol^{-1}. The values of $T\Delta\varepsilon/\chi$ calculated from equation (13) are shown in *Figure 9a*.

In case (ii), from equations (10) and (12), $T\Delta\varepsilon/\chi$ is given by:

$$\frac{T\Delta\varepsilon}{\chi}=\frac{4\pi}{3k}KN_0\mu_0^2\operatorname{sech}^2\left(\frac{\Delta G}{2kT}\right)\times\left[N_s\tanh^2\left(\frac{\Delta g}{2kT}\right)+\operatorname{sech}^2\left(\frac{\Delta g}{2kT}\right)\right] \tag{20}$$

In the same way as case (i), the following relations between parameters are obtained:

$$\Delta V/\Delta U=\Delta v/\Delta u \tag{21}$$

$$\frac{\Delta U}{2kT_0}\tanh\left(\frac{\Delta U}{2kT_0}\right)=\frac{\Delta u}{2kT_0}(N_s-1)\tanh\left(\frac{\Delta u}{2kT_0}\right)\times\operatorname{sech}^2\left(\frac{\Delta u}{2kT_0}\right)\Big/\left[(N_s-1)\tanh^2\left(\frac{\Delta u}{2kT_0}\right)+1\right] \tag{22}$$

$$\theta=\Delta U/T_0\Delta V \tag{23}$$

By fitting the calculated values to the experimental ones at P_{max}, we obtain the values of parameters as

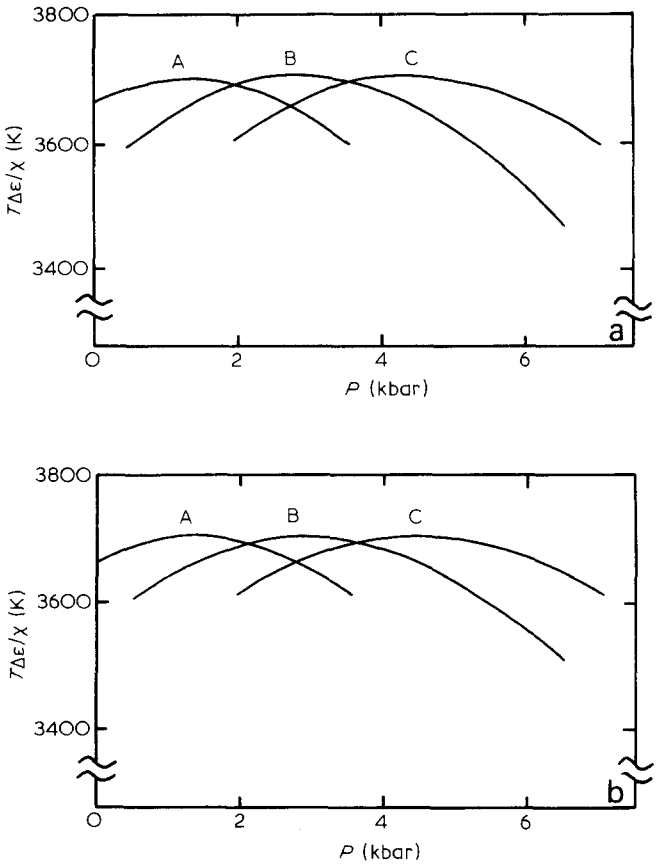

Figure 9 Calculated results of $T\Delta\varepsilon/\chi$: (a) case (i) and (b) case (ii). Curve A, 120°C; B, 160°C; C, 200°C. Parameter values are given in the text

$\Delta U = 1.3$ kcal mol^{-1}, $\Delta V = 3.9$ cm^3 mol^{-1}, $\Delta u = 0.92$ kcal mol^{-1} and $\Delta v = 2.8$ cm^3 mol^{-1}. The calculated results of $T\Delta\varepsilon/\chi$ are shown in *Figure 9b*.

No significant difference is seen in *Figures 9a* and *b*. Therefore, we cannot decide which case is preferable for the α relaxation.

The parameter values obtained are 5–20% of the activation parameters and so they are considered reasonable values. The calculated results explain the experimental ones, but the pressure dependence of $T\Delta\varepsilon/\chi$ is much smaller than the experimental results. The discrepancy may be due to the approximations used to derive equations (17) and (22).

We can check the alternatives of these two cases by examining the dependence of $T\Delta\varepsilon/\chi$ on N_s. Nakagawa and Ishida[14] reported that, at atmospheric pressure, the dielectric increment increases linearly with the lamellar thickness but the dielectric increment does not become zero by linear extrapolation of the lamellar thickness to zero. Their results may indicate that the present two cases coexist in the α relaxation. If these two cases are mixed, we cannot determine all the parameters by the present method because the data available are insufficient.

Structural analyses recently reported suggest that various disordered structures exist in crystal form II of PVDF[15,16]; these reports justify the present treatments. The dynamical mechanisms of the polarization along the molecular axis are examined by a kink propagation and the activation energy obtained by the calculations agrees with the experimental results[17].

CONCLUSIONS

The molecular motion causing the α relaxation in crystal form II of PVDF is essentially the one that changes $TGT\bar{G}$ conformation into $\bar{G}TGT$ one. This molecular motion occurs throughout the chains in crystallites. Since the metastable conformations exist together with the most stable ones in a chain, the dipole moment of one chain decreases with increasing temperature and decreasing pressure. As a result, the dielectric increment shows a maximum with respect to pressure and temperature.

ACKNOWLEDGEMENTS

The author would like to express his sincere thanks to Professor K. Asai and Dr H. Miyaji of Kyoto University for helpful advice and encouragement throughtout this work. The author also wishes to thank Dr N. Murayama of Kureha Chemical Ind. Co. Ltd for supplying the material.

APPENDIX

When each chain is assumed to be independent and has a different value of dipole moment, $N\mu^2$ in equation (5) should be written as:

$$N\langle\mu^2\rangle = N\sum_{i=1}^{N_s}\mu_i\sum_{j=1}^{N_s}\mu_j = N\left(N_s\mu_0^2 + 2\left\langle\sum_{1\le i<j\le N_s}\right\rangle\mu_i\mu_j\right) \tag{A.1}$$

where N_s is the number of segments per chain and μ_i is the dipole moment of the ith segment in a chain which equals $+\mu_0$ or $-\mu_0$. We consider the following situations. (1) Up state (1-state), the segment of which has a dipole moment of $+\mu_0$, is the ground state. (2) Down state (2-state), the segment of which has a dipole moment of $-\mu_0$, has a higher energy than up state by Δg. (3) Between the up state sequence and the down state one, a defect should intervene and the defect formation energy W is necessary.

Under these conditions, we regard the arrangements of the segments in a chain to be described by the simple Markov process. When the transition probability from i-state to j-state is written as p_{ij} $(i, j = 1, 2)$, from the definition of the probabilities

$$\sum_{j=1}^{2} p_{ij} = 1$$

the probability transition matrix **P** can be expressed by:

$$\mathbf{P} = \begin{pmatrix} 1-p & p \\ q & 1-q \end{pmatrix} \tag{A.2}$$

From the above conditions, p and q are given by:

$$\frac{p}{1-p} = e^{-(\Delta g + W)/RT} \qquad \frac{q}{1-q} = e^{-(W-\Delta g)/kT}$$

and hence:

$$p = (1 + e^{(\Delta g + W)/kT})^{-1}$$
$$q = (1 + e^{(W-\Delta g)/lT})^{-1} \tag{A.3}$$

Then from equation (A.1), $N\langle\mu^2\rangle$ can be expressed as follows:

$$N\langle\mu^2\rangle = N\left[N_s\mu_0^2 + 2\mu_0^2 \sum_{1\le i<j\le N_s} (\omega_1,\omega_2)\mathbf{P}^i\mathbf{U}\mathbf{P}^{j-i}\mathbf{U}\mathbf{P}^{N_s-j}\begin{pmatrix}1\\1\end{pmatrix}\right] \tag{A.4}$$

where the matrix $\mathbf{U}$ is given by

$$\mathbf{U} = \begin{pmatrix}1 & 0\\ 0 & -1\end{pmatrix} \tag{A.5}$$

and the initial vector (ω_1, ω_2) is assumed to be given by the fractions of up segment and down segment, respectively, that is:

$$\omega_1 = \frac{q}{p+q} \qquad \omega_2 = \frac{p}{p+q} \tag{A.6}$$

Since $\mathbf{P}^m$ can be calculated to be:

$$\mathbf{P}^m = \frac{1}{p+q}\begin{pmatrix}q & p\\ q & p\end{pmatrix} + \frac{(1-p-q)^m}{p+q}\begin{pmatrix}p & -p\\ q & -q\end{pmatrix} \tag{A.7}$$

the sum in equation (A.4) is given by:

$$\begin{aligned}\sum_{1\le i<j\le N_s} (\omega_1,\omega_2)\mathbf{P}^i\mathbf{U}\mathbf{P}^{j-i}\mathbf{U}\mathbf{P}^{N_s-1}\begin{pmatrix}1\\1\end{pmatrix}&\\ = \tfrac{1}{2}N_s(N_s-1)\left(\frac{p-q}{p+q}\right)^2&\\ +(N_s-1)\frac{4pq(1-p-q)}{(p+q)^3}&\\ -\frac{4pq(1-p-q)^2}{(p+q)^4}[1-(1-p-q)^{N_s-1}]&\end{aligned} \tag{A.8}$$

Substituting into (A.4) and from $NN_s = N_0$, we obtain:

$$N\langle\mu^2\rangle = N_0\mu_0^2\left[N_s\left(\frac{p-q}{p+q}\right)^2 + \frac{4pq(2-p-q)}{(p+q)^3} - \frac{1}{N_s}\frac{8pq(1-p-q)}{(p+q)^4}[1-(1-p-q)^{N_s}]\right] \tag{A.9}$$

REFERENCES

1 Hoffman, J. D., Williams, G. and Passaglia, E. *J. Polym. Sci. C* 1966, **14**, 173
2 Hoffman, J. D. and Pfeiffer, H. G. *J. Chem. Phys.* 1954, **22**, 132
3 Sayre, J. A., Swanson, S. R. and Boyd, R. H. *J. Polym. Sci., Polym. Phys. Edn.* 1978, **16**, 1739
4 Boyd, R. H. and Sayre, J. A. *J. Polym. Sci., Polym. Phys. Edn.* 1979, **17**, 1627
5 Miyamoto, Y., Miyaji, H. and Asai, K. *J. Polym. Sci., Polym. Phys. Edn.* 1980, **18**, 579
6 Nakagawa, K. and Ishida, Y. *Kolloid. Z. Z. Polym.* 1973, **251**, 103
7 Tanaka, H., Takayama, K., Okamoto, T. and Takemura, T. *Polym. J.* 1982, **14**, 719
8 Yano, S., Tadano, K. Aoki, K. and Koizumi, N. *J. Polym. Sci., Polym. Phys. Edn.* 1974, **12**, 1875
9 Sasabe, H., Researches on the Electrotechnical Laboratory, 1971, no. 721
10 Yano, S. *J. Polym. Sci. A-2* 1970, **8**, 1057
11 Hasegawa, R., Takahashi, Y., Chatani, Y. and Tadokoro, H. *Polym. J.* 1972, **3**, 600
12 Scholte, Th. G. *Physica* 1949, **15**, 436
13 Böttcher, C. J. F. 'Theory of Electric Polarization', Elsevier, New York, 1952, Ch. 3
14 Nakagawa, K. and Ishida, Y. *J. Polym. Sci., Polym. Phys. Edn.* 1973, **11**, 1503
15 Takahashi, Y. and Tadokoro, H. *Macromolecules* 1980, **13**, 1317
16 Bachmann, M. A. and Lando, J. B. *Macromolecules* 1981, **14**, 40
17 Clark, J. D., Taylor, P. L. Hopfinger, A. J. *J. Appl. Phys.* 1981, **52**, 5903